



Journal of Applied Sciences

ISSN 1812-5654

science
alert

ANSI*net*
an open access publisher
<http://ansinet.com>

Numerical Analysis of Structural Response and Attenuation Law of Vibration Caused by Moving Trains

Peng Chang, Qiangjun Li and Weiguo Yang
School of Civil Engineering, Beijing Jiaotong University, Beijing, 100044, China

Abstract: Vibration caused by train is one of main vibration types in the traffic environment incentive. Vibration transmitted through the surrounding soil and other media and affects its surroundings. Due to the different vibration nature and building foundations, the vibration attenuation shows different characteristics when wave passing from the source to the internal structure. Even sometimes, there will be amplification effect appeared. Therefore, it is necessary for transport routes and adjacent buildings to take isolation measures to ensure the safety of buildings. A seven-story museum building was used for the study and three-dimensional finite element model was established. Numerical simulations were completed for the structural response and there are four urban rail transit lines beneath the structure. And further, the attenuation laws of structural response under the rail vibration excitation are discussed. According to finite element analysis results, the train speed, the tunnel depth and the floating panels are the main factors affecting the response. When the speed of the train through the museum section was changed from 160-90 km h⁻¹, the acceleration of the upper structure reduces by 31.5% and the velocity reduces by 36%. After considering various measures, structural response can be controlled to ensure structural safety and suitability.

Key words: Tunnel, environmental vibration excitation, structural response, attenuation, numerical analysis

INTRODUCTION

The propagation of wave caused by a variety of vibration source in the environment spread around through the soil and other media and it produce a variety of effects to its surroundings. It would affect people's normal life and the suitability of the building when the vibration wave transmitted to the structures (Chen *et al.*, 2011). Due to the vibration properties, building foundations and type of structures are different, the vibration attenuation amount is in various status (Ju and Lin, 2004). Even the vibration would be amplified if vibration wave spread from the outside to the inside (Bata, 1985). This spread is difficult to be illustrated with a more consistent delivery mode. Structural vibration caused by the train tracks spread through the surrounding strata, then further induce neighboring buildings and underground structures and it seriously affects the structural safety and the use of performance of buildings (Walker and Chan, 1996). For example, in the Czech Republic, cracks were produced in masonry structure nearly a busy road and a rail lines because of the vehicle vibration (Yang *et al.*, 1999). In Prague, Haast Pass, Huosuo Fu and other places, ancient church collapsed because of the cracks were expanding. The above project examples show that it is necessary to take measures though shocking absorption and vibrational isolation to ensure the safety and the using performance of buildings (Fujikake, 1986).

As city's growing, rail transportation has been getting the rapid development. Then vibration pollution problem is getting people's attention. Domestic and foreign researchers have carried out in-depth study on the overload from rail transportation causing the nearby environment. For example, Through the establishment of three-dimensional finite element model, some research were do that the overload frequency of the train has certain effect on the surrounding soil. Ju *et al.* (2007), by the means of the experiments, studied the vibration of the soil when the train goes around. Xia *et al.* (1999), gave a review of the instructions about the vibration problems caused by the train overload and propose a variety of measures to reduce isolation. Xia *et al.* (2004) by field measurement, study the vibration effects of the train overload on the surrounding buildings.

The thesis puts a seven-story museum building as the research object, conducting for the numerical simulations about the impact on the structure. A 3D finite element numerical model with four urban rail transit line under the structure is established. The response of the structure and decay law under the track vibration excitation are studied. And the results provide technical basis for similar engineering problems.

NUMERICAL ANALYSIS MODEL

The model was build and meshed in the ansys program according to the topographic map and

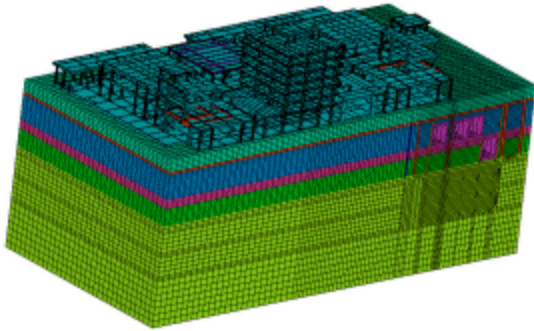


Fig. 1: Finite element model

designing scheme. The model contains 181712 nodes and 123022 elements which include 4980 beam elements, 1984 shell elements and 166058 solid elements. The figure of the finite element model is shown in Fig. 1.

Choice of the soil dimension: The dimension of the element can be analyzed by the dispersion phenomenon in the soil which is caused by the divisions of elements. And the phase velocity changing with the vibration frequency is called as the dispersion phenomenon. For a planar finite element model divided by rectangles, the dispersion equation of the fluctuation can be expressed as Eq. 1:

$$abQ_1\omega^2 - c^2 \frac{2}{3\lambda} (Q_2 + Q_3) = 0 \quad (1)$$

Where:

$$Q_1 = \frac{4}{9} [4 + 2\cos k_1 \Delta x + 2\cos k_2 \Delta y + \cos k_1 \Delta x \cos k_2 \Delta y]$$

$$Q_2 = (1 + \lambda^2) + (\lambda^2 - 2) \cos k_1 \Delta x$$

$$Q_3 = (1 + 2\lambda^2) \cos k_1 \Delta y + (1 + \lambda^2) \cos k_1 \Delta x \cos k_2 \Delta x$$

In this equation: a is the half of element length Δx along the x-axis; b is the half of element length Δy along the y-axis; ω is the circular frequency of the vibrating load; c is the wave velocity in the soil; $\lambda = a/b$; k_1 and k_2 are the numbers of the waves along the x-axis and y-axis, respectively, where $k_1 = k \cdot \cos \theta$, $k_2 = k \cdot \sin \theta$, k is the number of waves along any direction in the x-y plane, $k = \omega/c_p$; c_p is the phase velocity of the wave; θ is the angle between the direction of wave travel and the x-axis.

It is shown in the theory and practice that the error can usually be ignored by using Finite Element Modeling (FEM) instead of the continuous medium model, when the meshing size of FEM is small enough. The wave propagation in models of two and three dimensions will bring some new problems besides of the dispersion and the cutoff frequency in the one-dimensional discrete model. Therefore, it should make the element mesh size small enough when the transient wave propagation problems were analyzed. Some research (Degrande *et al.*, 2000) indicates when the unit length of the side is approaching the vibration overload action point, it can obtain satisfied results as long as its length is less than $\lambda s/6$. According to different boundary conditions, it demonstrates that the satisfied result can be received when the dimension of the cell size is set between $\lambda s/12$ and $\lambda s/8$. When the ratio between the maximum size unit and the shortest wavelength is set by $1/4$, the higher calculation accuracy can be worked out.

In summary, in order to achieve a reliable accuracy, the element length was chosen between 0.8 to 3 meters in the finite element model.

Artificial boundary: The free boundary theory should be considered first when the fluctuant problems of the soil we solved. The simulation will distort by using the finite discrete model to simulate infinite ground, because of wave reflection on the artificial interception boundary. Bringing in the artificial boundary is the way to solve this problem. So many researchers have proposed various artificial boundaries to solve the wave reflection problem on the boundary in the model.

The viscous boundary is widely used in a long time because of its clear concept and ease of application. While the viscous boundary is based on the one-dimensional wave theory, there will be a large error if it is simply extended to the multi-dimensional case. To overcome the disadvantages above, Deeks and Randolph (1994) and Liu *et al.* (2005, 2006) established two-dimensional viscoelastic medium artificial boundaries based on cylindrical wave equations. Compared with viscous boundaries, the advantage of this theory is that it cannot only simulate the elastic recovery properties of the semi-infinite medium beyond the artificial boundary but also it has a good stability in both high-frequency and low-frequency.

Two-dimensional viscoelastic medium dynamical artificial boundaries can be equivalent to installing continuously distributed and parallel spring-damper systems on the artificial truncation boundaries, where

elasticity coefficient K_b of the spring element and damping coefficient C_b of the viscous damper are calculated as follows:

$$K_b = \alpha \frac{G}{R} \quad (2)$$

$$C_b = \rho c \quad (3)$$

where, ρ and G are represented as mass density and shear modulus, respectively. R is represented as the distance between the source of the wave and the artificial boundary. C is represented as the wave velocity, we choose the p-wave velocity C_p as the centripetal artificial boundary c . Parameter is represented as the value of the type and setting-up direction of the artificial boundary.

Viscoelastic medium dynamical artificial boundary can be combined with Finite Element Method conveniently. It is only needed to set up elastic and damper elements in parallel in the centripetal directions and tangential directions of artificial boundary nodes in the finite element model.

Distribution of the control points in the model: Five control points include two (1 and 2) on the top of basement (The Air defense fortifications) and three (3, 4 and 5) on the floor 5 (Elevation of 28.2 m) were chosen in this model as the result of computation. The figure of their location as followed.

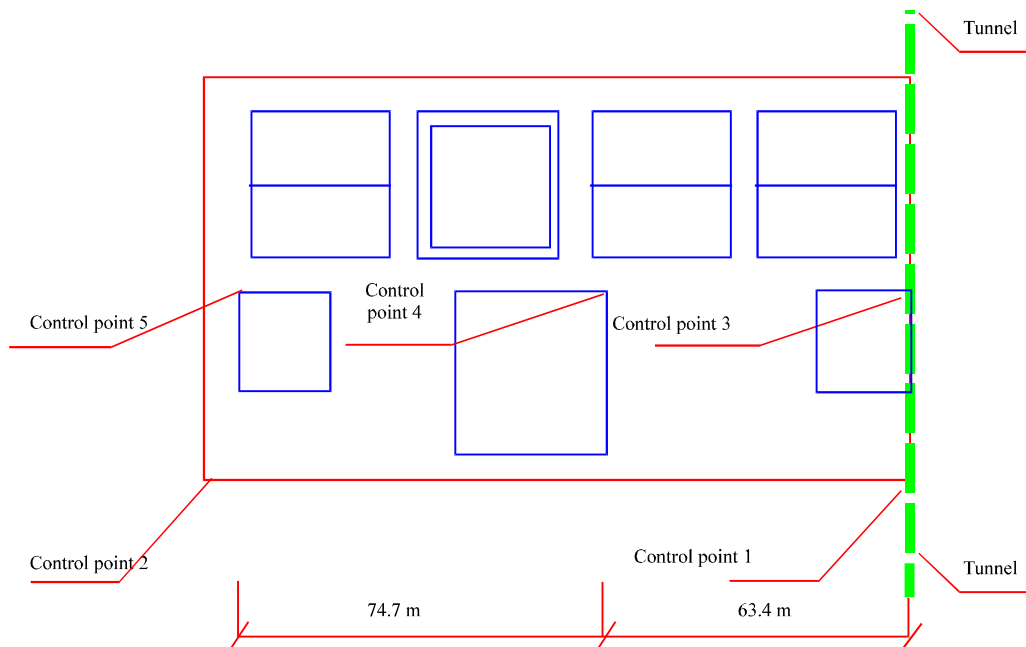


Fig. 2: Distribution map of control point

STRUCTURAL RESPONSE

Selection of calculation parameters: In order to studying the effect of vibration caused by different speed, different Tunnel wall thickness and floating slab, many working condition cases with different parameters are analyzed. And the speed is 160 and 90 km h⁻¹, the tunnel wall thickness is 100cm and 200cm and other including sitting floating slab or not:

- **CASE 0: (Original program):** Speed 160 km h⁻¹, 1 h tunnel wall thickness, not setting floating slab
- **CASE 1 (Reducing the train speed):** Speed 90 km h⁻¹, 1h tunnel wall thickness, not setting floating slab
- **CASE 2 (Floating slab):** Speed 160 km h⁻¹, 1h tunnel wall thickness, setting floating slab.
- **CASE (Increase the wall thickness):** Speed 160 km h⁻¹, 2 h tunnel wall thickness, not setting floating slab
- **CASE 4 (Comprehensive programs):** Speed 90 km h⁻¹, 2 h tunnel wall thickness, setting floating slab, deviating 30m from museum, 12m deep isolation trench, wave impeding block

Finite element analysis results of original design: The model of tunnel-soil body-museum is analyzed by the software of ansys program, so we can get its transient dynamic response. Under the original design

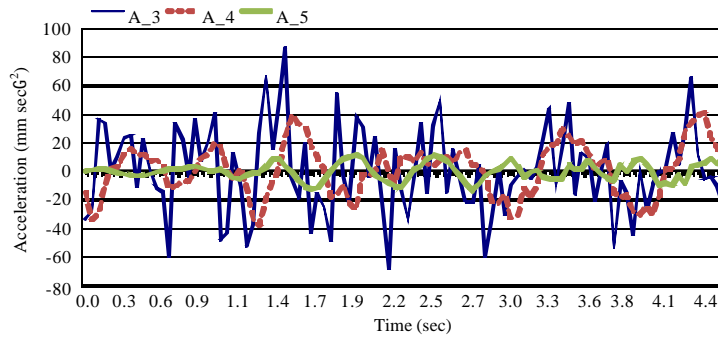


Fig. 3: Acceleration time-history curve of original design condition

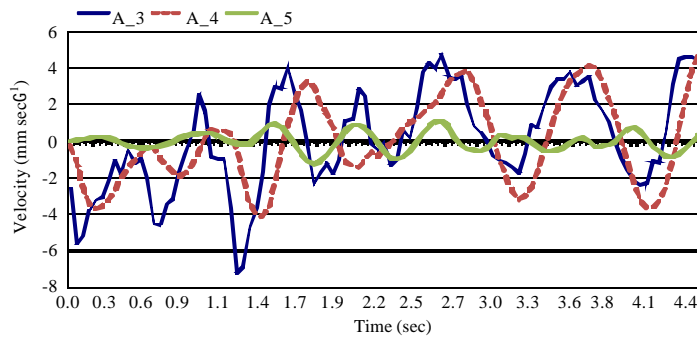


Fig. 4: Velocity time-history curve of original design condition

Table 1: A and V under original design case

Control	Point	1	2	3	4	5
A	Max	139	15.60	86.20	41.60	11.40
	Min	-129	-17.60	-68.10	-37.80	-13.20
	Amp.	269	33.20	154.40	79.40	24.60
V	Max	4.6	0.98	4.74	5.31	1.09
	Min	-8.1	-1.77	-7.20	-4.10	-1.23
	Amp.	12.8	2.76	11.90	9.40	2.32

case, the velocity and acceleration value of all control points as showed in Table 1.

The acceleration and velocity time-history curves of the point 3, 4 and 5 as showed in Fig 3 and 4.

Analyzing the results under other working case

Reducing the train speed: By comparing the analyze of case 1 and original design case, when the speed is 90 and 160 km h⁻¹, the acceleration and velocity time-history curves of the point 5 as showed in Fig 5 and 6.

Through the above all, if the speed of trains through the museum section dropped from 160-90 km h⁻¹, the acceleration peak-to-peak value of superstructure (28.2 m) decreasing from 154.43-105.78 mm sec⁻², approximately reduce 31.5%. The speed peak-to-peak value of superstructure decreasing from 11.94-7.64 mm sec⁻¹, approximately reduce 36.0%.

Setting floating slab in the museum section: By comparing the analyze of case 2 and original design case, whether there is a floating slab or not near the museum, the acceleration and velocity time-history curves of the point 3 and 5 as showed in Fig 7 and 8.

As can be seen from the above, if it is used the floating slab, the acceleration peak-to-peak value of superstructure decreasing from 154.43-71.00 mm sec⁻², approximately reduce 54.02%. The speed peak-to-peak value of superstructure which decrease from 11.94-4.97 mm sec⁻¹, approximately reduce 58.38%.

Increase the wall thickness of the tunnel: By comparing the analyze of case 3 and original design case, when increase the wall thickness of the tunnel twice as the original, the acceleration and velocity time-history curves of the point 3 and 5 as showed in Fig 9 and 10.

From the above curves can see, if doubling the tunnel wall thickness, the acceleration peak-to-peak value of superstructure decreasing from 154.43-42.40 mm sec⁻², approximately reduce 72.54%. The speed peak-to-peak value of superstructure which decrease from 11.94-3.04 mm sec⁻¹, approximately reduce 74.54%.

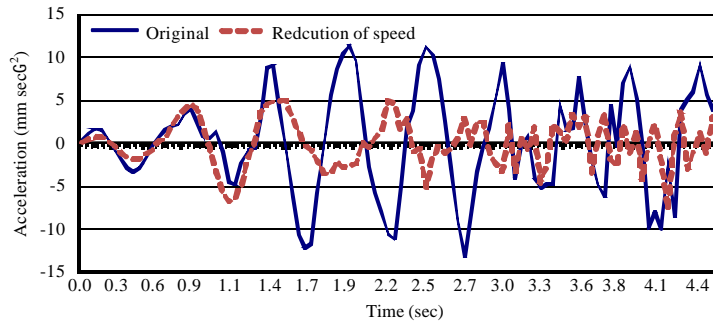


Fig. 5: Acceleration time-history curve by different speed excitation

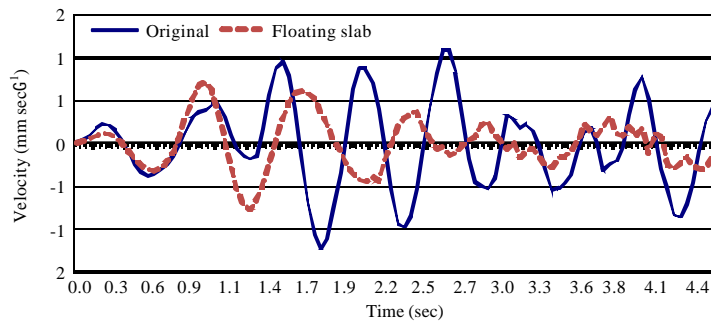


Fig. 6: Velocity time-history curve by different speed excitation

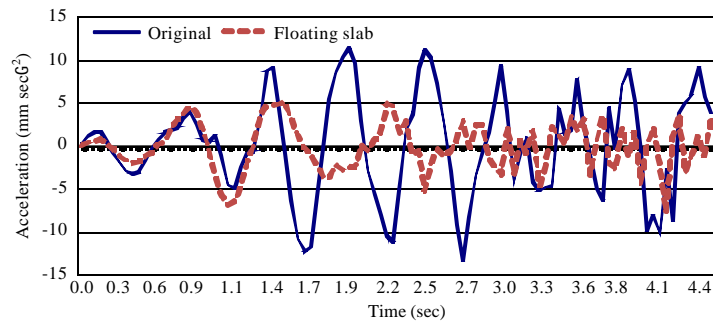


Fig. 7: Acceleration time-history curve by having floating slab or not

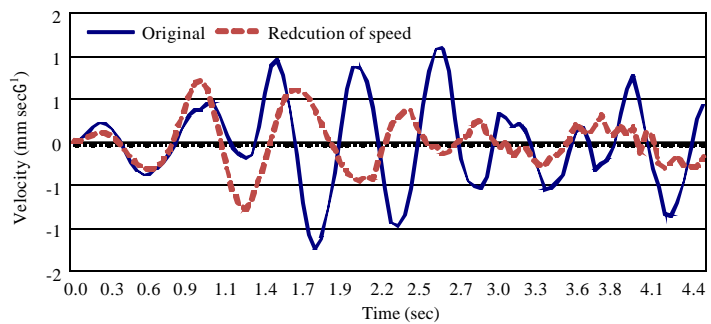


Fig. 8: Velocity time-history curve by having floating slab or not

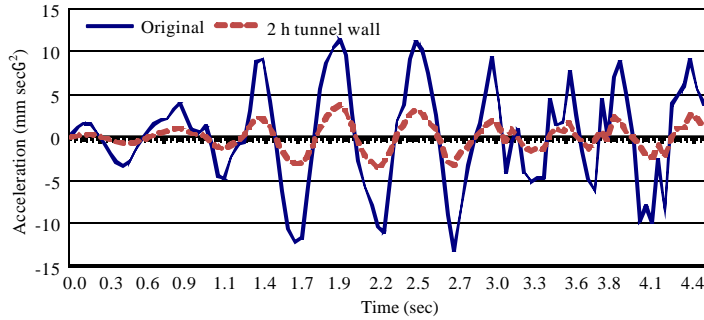


Fig. 9: Acceleration time-history curve by different tunnel wall thickness

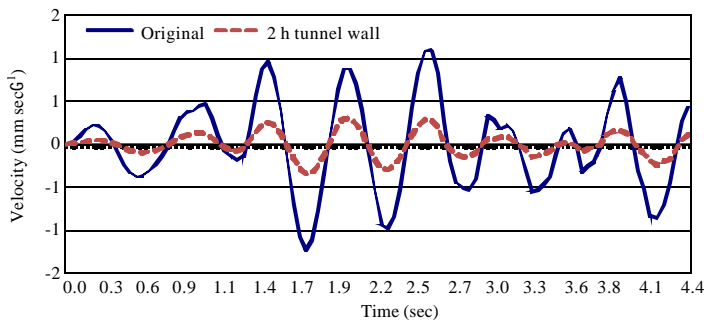


Fig. 10: Velocity time-history curve by different tunnel wall thickness

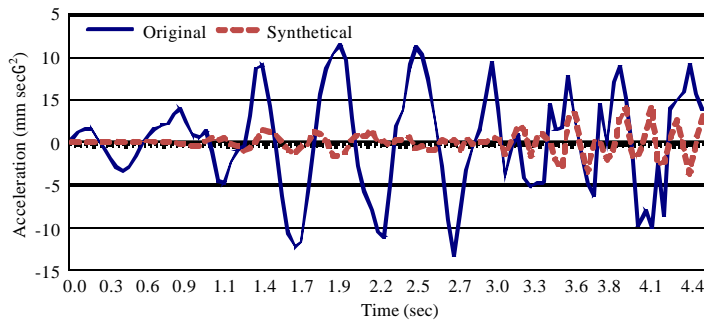


Fig. 11: Acceleration time-history curve of original and comprehensive case

Comprehensive case: By comparing the analyze of case 4 and original design case, if reducing the speed from 160-90 km h⁻¹, increasing the wall thickness from 100- 200 cm, deviating 30m from museum, setting floating slab,12m deep isolation trench and wave impeding block, the acceleration and velocity time-history curves of the point 3 and 5 as showed in Fig 11 and 12.

Above all, if integrated application of various means are used to reduce the vibration source excitation input, the results display that the acceleration peak-to-peak value of superstructure decreasing from 154.43-10.76 mm sec⁻², approximately reduce 93.03%. The

speed peak-to-peak value of superstructure which decrease from 11.94-0.43 mm sec⁻¹, approximately reduce 93.44%.

ATTENUATION LAW OF VIBRATION RESPONSE

Attenuation coming from vibration source: Based on the result of numerical model, if the train speed reaches 160 km h⁻¹ through the museum section, the maximum acceleration and acceleration peak-to-peak value of the superstructure is 139.96 and 269.35 mm sec⁻² and the maximum velocity and velocity peak-peak value is 8.19 and 12.84 mm sec⁻¹.

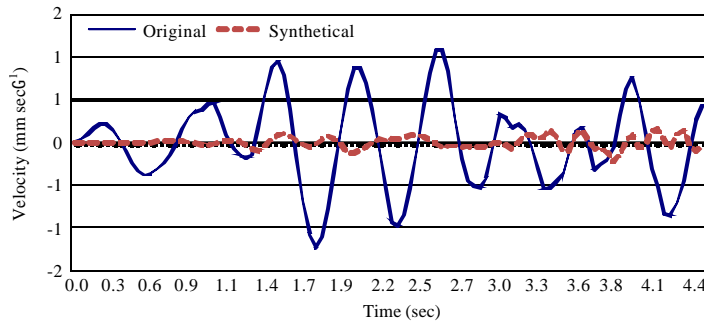


Fig. 12: Velocity time-history curve of original and comprehensive case

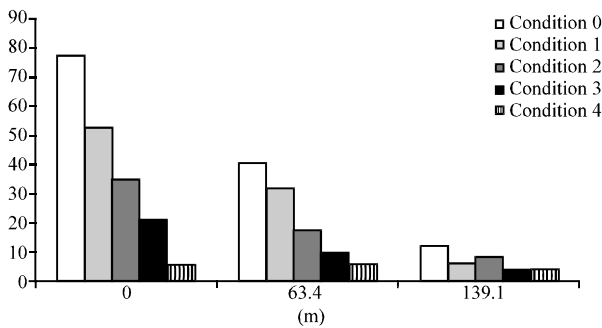


Fig. 13: Half of the acceleration peak-to-peak value (mm sec⁻²)

Table 2: Simulated results of the control point 1

	Acceleration (mm sec ⁻²)			Vibration level (dB)
	Max	Min	Amp./2	
Case 0	139.96	-129.38	134.67	102.59
Case 1	61.30	-84.20	72.25	97.18
Case 2	43.70	-35.64	39.67	91.97
Case 3	67.37	-106.89	87.13	98.80
Case 4	9.82	-7.00	8.41	78.5

While the train speed drops to 90 km h⁻¹, the maximum acceleration and acceleration peak-to-peak value of the superstructure is 84.20 and 145.50 mm sec⁻², meanwhile, the maximum velocity and velocity peak-peak value is 4.82 and 8.08 mm sec⁻¹.

If fixing a floating slab on the rail, the maximum acceleration and acceleration peak-to-peak value of the superstructure is 43.70 and 79.34 mm sec⁻², meanwhile, the maximum velocity and velocity peak-peak value is 3.94 and 7.05 mm sec⁻¹.

On the base above, while doubling the tunnel wall thickness, the maximum acceleration and acceleration peak-to-peak value of the superstructure is 106.89 and 174.26 mm sec⁻², meanwhile, the maximum velocity and velocity peak-peak value is 1.88 and 3.09 mm sec⁻¹.

Under the Comprehensive case, including reducing the speed, deviating 30 m from museum, setting floating

slab, 12 m deep isolation trench and wave impeding block, the maximum acceleration and acceleration peak-to-peak value of the superstructure is 9.82 and 16.82 mm sec⁻², meanwhile, the maximum velocity and velocity peak-peak value is 0.46 and 0.77 mm sec⁻¹.

Museum of tunnels in vibration control points of the finite element analysis results as showed in Table 2.

Attenuation in the space: Under the original scheme, the acceleration of museum near the tunnel is 86.25 mm sec⁻² and the velocity is 7.2 mm sec⁻¹. Correspondingly, the acceleration of distal end is 13.26 mm sec⁻², and the velocity is 1.23 mm sec⁻¹.

While the train goes through the museum section with reducing speed, the acceleration of museum near the tunnel is 53.01 mm sec⁻² and the velocity is 4.46 mm sec⁻¹. Correspondingly, the acceleration of distal end is 7.70 and the velocity is 0.78 mm sec⁻¹.

If using floating slab, the acceleration of museum near the tunnel is 35.72 mm sec⁻² and the velocity is 2.67 mm sec⁻¹. Correspondingly, the acceleration of distal end is 8.25 mm sec⁻² and the velocity is 0.41 mm sec⁻¹.

And if the tunnel wall thickening, the acceleration of museum near the tunnel is 22.18 mm sec⁻² and the velocity is 1.75 mm sec⁻¹. Correspondingly, the acceleration of distal end is 3.80 mm sec⁻² and the velocity is 0.34 mm sec⁻¹.

Under the comprehensive case, including reducing the speed, deviating 30 m from museum, setting floating slab, 12 m deep isolation trench and wave impeding block, the acceleration of museum near the tunnel is 5.66 mm sec⁻² and the velocity is 0.43 mm sec⁻¹. Correspondingly, the acceleration of distal end is 4.32 mm sec⁻² and the velocity is 0.22 mm sec⁻¹.

The results of the finite element analysis which give the attenuation law along the perpendicular direction of tunnel are showed in Fig. 13.

CONCLUSION

The thesis puts a seven-story museum building as the research object, establishing a 3D finite element numerical model. According to finite element analysis results, the conclusions as follows:

- When the speed of the train through the museum section was changed from 160-90 km h⁻¹, the acceleration of the upper structure reduces by 31.5% and the velocity reduces by 36%. When the floating slabs were used on the rail near the museum, the acceleration of the upper structure decreases 54.02% and the velocity reduces 58.38%; if the tunnel wall near the museum was thickened more one times, the acceleration of the upper structure will decrease 72.54% and the velocity will reduce 74.54%
- When the train goes through the museum section under the original program, in the direction perpendicular to the tunnel, the museum ends up 84.02% decay acceleration, the velocity decreases 80.54%
- Compared with the original design and considering comprehensive case, the acceleration of the upper structure decreases 93.03% and the velocity reduces 94.44%
- Difference in distance from the tunnel contribute to the distinction of the vibration attenuation of museum. In addition, under different cases, the distal end (leave the tunnel wall at 138.1 m) and the proximal end (above the tunnel) of the vibration level is different between 13 and 18 dB

ACKNOWLEDGEMENTS

This study was supported by the Fundamental Research Funds for the Central Universities under Grant No. 2013JBM066, the National Nature Science Foundation of China under Grant No. 51078028 and the Doctoral Fund of Ministry of Education of China under Grant No. 20100009110015.

REFERENCES

Bata, M., 1985. Effect on building of vibrations caused by traffic. *Build. Sci.*, 99: 1-2.

- Chen, Y., S. Lin, Y. Shen, S. Lin and J. Lu, 2011. Analysis model of ground vibration propagation for high-speed trains. *Geo-Frontiers*, 2011: 3748-3755.
- Deeks, A.J. and M.F. Randolph, 1994. Axisymmetric time-domain transmitting boundaries. *J. Engine. Mech.*, 120: 25-42.
- Degrande, G., G. Lombaert, G. Degr and G. Lombaert, 2000. High-speed train induced free field vibrations: In situ measurements and numerical modelling. *Proc. Wave.*, 2000: 29-42.
- Fujikake, T.A., 1986. A prediction method for the propagation of ground vibration from railway trains. *Sound Vibrat.*, 111: 289-297.
- Ju, S., H. Lin and T. Chen, 2007. Studying characteristics of train-induced ground vibrations adjacent to an elevated railway by field experiments. *J. Geotech. Geoenviron Engine*, 133: 1302-1307.
- Ju, S.H. and H.T. Lin, 2004. Analysis of train-induced vibrations and vibration reduction schemes above and below critical Rayleigh speeds by finite element method. *Soil Dyn. Earthquake Engine.*, 24: 993-1002.
- Liu, J.B., G. Yin and Y.X. Du, 2006. Consistent viscous-spring artificial boundaries and viscous-spring boundary elements. *Chinese J. Geotech. Engine.*, 9: 55-63.
- Liu, J.B., Z.Y. Wang, X.L. Du and Y.X. Du, 2005. Three dimensional viscous-spring artificial boundaries in time domain for wave motion problems. *Engine. Mech.*, 22: 46-51.
- Walker, J.G. and M.F.K. Chan, 1996. Human response to structurally radiated noise due to underground railway operations. *J. Sound Vibrat.*, 193: 49-63.
- Xia, H., N. Zhang and Y.M. Cao, 2004. Experimental study of train-induced vibrations of ground and nearby buildings. *J. China Railway Soc.*, 26: 43-48.
- Xia, H., W. Xuan and Y. Darning, 1999. Environmental vibration induced by urban rail transit system. *J. North. Jiaotong Univ.*, 23: 65-73.
- Yang, G., H. Zhang and H. Xia, 1999. The attenuation behavior of ground vibration under bridge caused by moving trains. *J. North. Jiaotong Univ.*, 23: 54-58.